J. F. Ziegler
M. Berkenblit
T. B. Light
K. C. Park
A. Reisman

Nuclear Backscattering Analysis of $Nb-Nb_2O_5-Bi$ Structure

Abstract: The technique of nuclear backscattering has been used to analyze the interface reactions of $Nb-Nb_2O_5-Bi$ multilayer films. This new analytical technique is explained in detail. It has been concluded that the drastic and erratic changes in the electrical properties of niobium oxide switchable resistor devices that take place at 450°C are associated with the gross migration of oxygen from the oxide to the niobium layer. The accompanying reactions of bismuth with the oxide are relatively moderate, diffusing less than 3×10^{11} atoms/cm^2 of bismuth into the oxide layer.

Introduction

Thin films of amorphous Nb_2O_5 in $Nb-Nb_2O_5-Bi$ structures exhibit bistable switching and memory effects after being formed electrically [1-3]. The forming involves an irreversible breakdown of the oxide to a low-resistance state and has usually been accomplished by the application of a relatively high positive voltage (2.1 to 2.7 MV/cm) to the Bi electrode. Controlled thermal treatment of amorphous Nb_2O_5 eliminates the need for a catastrophic electrical breakdown for forming and produces a selectively reduced oxide, which requires only a minimal forming voltage. The role of Bi in this forming process has been discussed in Ref. 3.

This communication reports the results of an investigation in which the technique of nuclear backscattering was used to analyze the effects of thermal treatment on the multilayered $Nb-Nb_2O_5-Bi$ structure. In particular, the technique has provided detailed information about the migration of oxygen and bismuth in the system.

Nuclear backscattering

- *Physical basis for analysis*

In the nuclear backscattering method of surface analysis, a beam of high-energy ions is projected into a target material. A few of these ions come close enough to the nuclei of atoms in the target to undergo a severe repulsive scattering effect that causes them to come back out of the target (see Fig. 1). When the target atom recoils from the impact of collision, it absorbs some of the ion's energy and the ion leaves the target with less than its incident energy.

This recoil absorption by the target atom is the heart of nuclear backscattering analysis. The different elements of a target material absorb different fractions of the projectile ion's energy. Heavy elements, such as bismuth, absorb very little energy—as little as eight percent. Light elements, such as oxygen, can absorb as much as 65 percent of the ion's energy. The difference between the energy of the projectile and the energy of a backscattered ion depends on the mass of the scattering atom. Thus, by measuring the energies of backscattered ions, one can identify the constituent elements of a complex thin film.

Another phenomenon besides collisions with target nuclei affects the energy of backscattered ions: the electron "sea" in a target material absorbs energy from projectile ions, both on their way into the material and on their way out. The absorption of energy by electrons is about 0.07 keV per monolayer of the target material (the exact value varies slightly from material to material). Thus, ions backscattered from collisions with atoms deep within the material have energies less than those backscattered from collisions with surface atoms of the same element.

Interpreting the energy spectrum of backscattered ions permits one to determine not only the atomic elements that were in collision with the ions, but also the depths of those elements in the target material. The energy spectrum can then be transformed into concentration-vs-depth profiles for each element of the target film.

- *Calculations used in analysis*

The calculations used in nuclear backscattering analysis have been described in several recent papers; e.g., [4,5]. The energy loss due to collision of a projectile ion with an atom on the surface of the target material is represented by

$$\frac{E_{\text{out}}}{E_{\text{in}}} = \left[\frac{M_1 \cos\theta + (M_2^2 - M_1^2 \sin^2\theta)^{1/2}}{M_1 + M_2}\right]^2, \qquad (1)$$

where E_{in} is the energy of the projectile ion, E_{out} is the energy of the backscattered ion, M_1 and M_2 are the masses of the ion and the target atom, respectively, and θ is the total angle of scatter. Solving Eq. (1) for a beam of He^4 ions projected at $E_{\text{in}} = 2500$ keV, and assuming a scattering angle of 160°, one obtains the following values of E_{out} for Bi, Nb, Al, and O, respectively: 2321, 2115, 1400, and 927 keV.

These values permit one to determine which peaks in a backscatter energy spectrum correspond to the known constituent elements of the target material. The peaks can then be analyzed to obtain concentration values for the elements. The number of atoms/cm^2 of a given element is calculated from

$$N = C / \, (d\sigma \, / \, d\Omega) \; Q \; d\Omega\,, \qquad (2)$$

where C is the number of ions backscattered from the element, Q is the total number of ions incident on the target during the course of an experiment, $d\Omega$ is the solid angle of the detector, and $d\sigma/d\Omega$ is the differential scattering cross section for the given detector angle. The scattering cross section is calculated from

$$\frac{d\sigma}{d\Omega} = \left(\frac{e^2 Z_1 Z_2}{2E_{\text{in}} \sin^2\theta}\right)^2 \frac{(\cos\theta + \{1 - [(M_1/M_2)\sin\theta]^2\}^{1/2})^2}{\{1 - [(M_1/M_2)\sin\theta]^2\}^{1/2}}, \qquad (3)$$

where e is the electronic charge, and Z_1 and Z_2 are the atomic numbers of the projectile ion and the target atom, respectively.

Experiments

- *Apparatus, sample structure, and thermal treatment*

The apparatus used for the experimental study is shown schematically in Fig. 1. It consists of a 2500-keV heavy-ion accelerator, a variable-angle target mount, and a silicon surface barrier detector. The detector angle is 5.525 millisteradians. A beam of monoenergetic He^4 ions is collimated and directed into the target. Although hydrogen could be used as a projectile, helium was preferred because its nuclear resonance effects occur at much higher energies than do those of hydrogen.

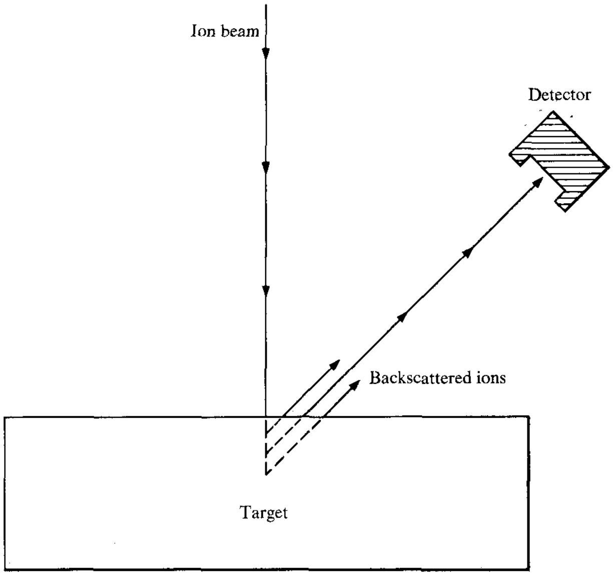

Figure 1 Schematic diagram of experimental nuclear backscattering apparatus. The ions in the incident beam penetrate the target, losing small amounts of energy as they pass through the electron "sea." A few ions approach close enough to atomic nuclei in the target to undergo collisions that cause them to scatter back out of the material. These backscattered ions are individually counted and their energies measured by a detector. The amount of energy possessed by a backscattered ion is related to the mass of the scattering element and its depth in the target.

Figure 2 Cross section of the Nb-Nb_2O_5-Bi structure that was analyzed. The Bi and Nb layers are used as electrical contacts to the oxide layer.

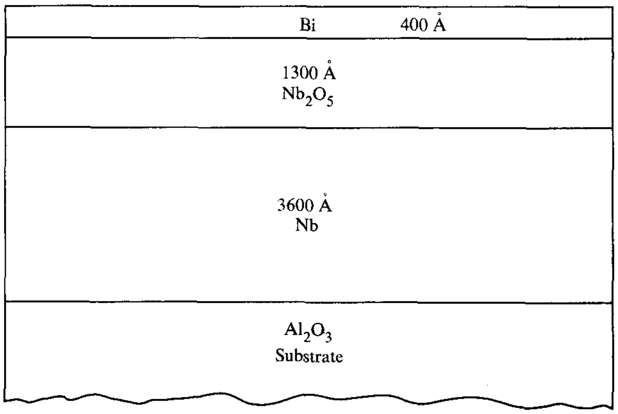

The structure of the target material is shown in Fig. 2. The structure and fabrication method are essentially the same as those reported by Basavaiah and Park [2]. The Nb base layer was deposited on an Al_2O_3 substrate by rf

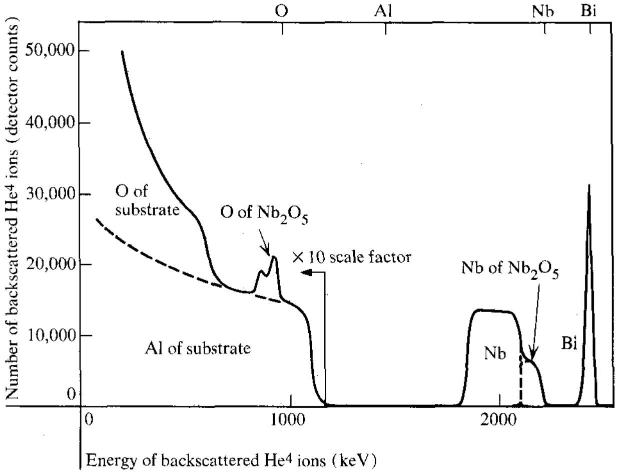

Figure 3 Typical backscatter energy spectrum from a sample having the dimensions shown in Fig. 2. The spectral peaks corresponding to the different target elements are separated from each other because the lighter nuclei absorb more energy in recoil than do the heavier nuclei, leaving the backscattered helium ions with less energy. Each spectral peak represents a concentration vs depth profile for an element in one of the target layers. The spread of energies under a peak results from the fact that backscattered ions lose a small amount of energy per unit distance traversed through the electrons in the target material. The projectile energy used to obtain this spectrum was 2500 keV.

sputtering, and the Nb_2O_5 layer was prepared by anodizing the Nb film in an ethylene glycol solution containing ammonium pentaborate. Then the structure was completed by depositing a Bi layer approximately 400 Å thick. The thickness of the oxide layers in the various samples studied ranged from 1000 to 1500 Å, and the Nb layers from 4000 to 6000 Å. X-ray and electron diffraction patterns of fresh oxide films showed no crystalline structure, indicating that the oxide was either amorphous or had a crystallite size of less than 20 Å.

Because the nuclear backscattering technique discussed here is a nondestructive method of analysis, the same sample can be used to obtain unambiguous information about the effects of thermal treatment on diffusion, reduction, and crystallization in the sample. Samples subjected to heat treatment were placed in an atmosphere of helium containing about 50 ppm of oxygen. The oxygen pressures were established by mixing oxygen with niobium-gettered helium. During the first five minutes of heat treatment, the temperature of the sample was raised to a value about 10°C below the desired annealing temperature. Then the temperature was increased to the annealing point during a period of thirty minutes. At the conclusion of the thermal treatment, the sample was pulled back into the cold portion of the furnace and allowed to cool to room temperature in the ambient gas.

• *Results*

In the early experimental runs the He^4 ions were projected into the targets at 2500 keV and the target table was positioned at an angle normal to the projectile beam. A typical energy spectrum from an unannealed sample is shown in Fig. 3. At the top border of the figure, index marks are drawn to indicate the surface backscatter energies calculated from Eq. (1) for the constituent elements. Comparing the locations of the marks with the locations of peaks in the spectrum permits one to correlate the peaks with the elements of the target material. Further interpretation of the spectrum is obtained by noting the difference between the energy at an index mark and the energy at a point on the corresponding spectral peak. The difference is proportional to the depth in the material at which the scattering event occurred. For example, ions backscattered from Nb atoms at the top of the Nb_2O_5 layer have energies offset from the Nb mark by an amount approximately equal to the half-width of the Bi peak in Fig. 3.

The accuracy of the energy spectrum is limited by the resolution of the experimental system—about 250 Å. Any film layers thinner than that will be represented on the spectrum by peaks with half-widths corresponding to 250 Å.

The accuracy of the concentration profiles derived from the backscatter energy spectrum is also affected by two phenomena of nuclear physics: 1) the stopping power of the absorbing target material and 2) resonance effects between the projectile ions and the target atoms. For a material having a uniform distribution of atoms, the shape of the spectrum shows an approximate $1/E$ dependence due to the stopping power. This dependence is clearly evident in Fig. 3 at the low-energy end of the spectrum, where the scattering events are attributed to collisions in the Al_2O_3 substrate. At higher energies the stopping power does not significantly affect the shape of the spectrum. In the analysis that follows, corrections have been made to account for stopping power, but these calculations are not discussed in this paper (see Ref. 6).

In Fig. 3, one also sees a double hump in the spectral peak that corresponds to ion collisions with oxygen in the Nb_2O_5 layer. The double hump is not an effect of oxygen concentration in that layer but, rather, results from the first nuclear scattering resonance between He^4 and O^{16}, which occurs at 2490 keV. In deriving concentration profiles, it is possible to correct for this effect by using complex theoretical calculations. However, it is more convenient to sidestep the problem by lowering the energy of the projectile beam to a value less than the resonance threshold.

To increase the accuracy of the analysis, two modifications to the experimental procedure described above were introduced. First, the ion beam energy was reduced to 2200 keV to avoid the $He^4 + O^{16}$ resonance. Second, the target was tilted from the beam by 60° to double the apparent thickness of the film layers to the beam. An energy spectrum resulting from these experimental modifications is shown in Fig. 4. Tilting the target decreased by a significant amount the energies of ions scattered from collisions in the Al_2O_3 substrate. Since the Nb_2O_5 layer was closer to the surface of the target, the spectral peak corresponding to the oxygen in the layer was not shifted as much; Fig. 4 shows that the peak occurs in a region having very few background counts. Hence, the accuracy of the oxygen concentration profile was increased. Figure 4 also shows that the lower energy of the incident ions removed the resonance effect from the oxygen peak.

Analysis

- *Niobium oxide*

A concentration profile of oxygen in the Nb_2O_5 layer is shown in Fig. 5. This profile was obtained from the data used to plot Fig. 4 by subtracting the background counts under the oxygen peak with a computer-aided least-squares fitting procedure. The background averaged 300 counts over the energy range under the peak and the peak height averaged about 1200 counts above the background. Integrating the area under the peak in Fig. 5 gave a total of 27,437 counts. This number was inserted into Eq. (2) from which a calculated value of 6.73×10^{17} atoms/cm^2 was obtained for the oxygen concentration. Dividing this value by 5.07×10^{22} atoms/cm^3, the assumed density of oxygen in the layer, gives a thickness of 1327 Å for the Nb_2O_5 layer.

The stoichiometry of the oxide was determined by comparing the number of oxygen and niobium counts at equivalent depths in the film and correcting for the differences in cross section. At the middle of the oxide layer, the ratio of oxygen to niobium atoms is

$$\frac{\mathrm{O}}{\mathrm{Nb}}=\frac{C_{\mathrm{O}}}{C_{\mathrm{Nb}}}\frac{\sigma_{\mathrm{Nb}}}{\sigma_{\mathrm{O}}}=\frac{1158}{13720}\,\frac{2.46\times10^{-24}}{8.32\times10^{-26}}=\frac{4.98}{2}.$$

Repeated experiments have shown the accuracy of this measurement to be seven percent.

The same sample used to obtain the profile of Fig. 5 was subjected to heat treatment at 375°C. The oxygen profile resulting from backscattering analysis of the treated sample appears in Fig. 6. The same calculations used to analyze the untreated sample showed that the oxide layer thickness was reduced to 1226 Å and that the oxygen to niobium ratio remained at approximately 5/2.

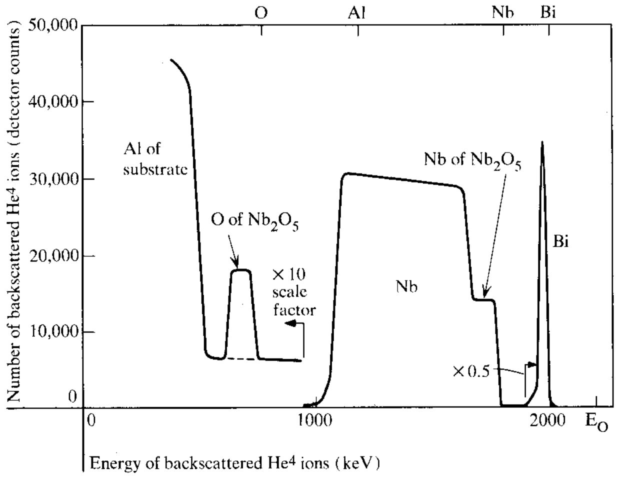

Figure 4 Energy spectrum obtained under modified experimental conditions. The projectile energy was reduced to 2200 keV to eliminate the resonance at 2490 keV, and the target was tilted by 60° to double its apparent thickness to the beam. In comparison with Fig. 3, the Al_2O_3 substrate spectrum is at lower energies, leaving the oxygen of the Nb_2O_5 layer on a lower background and increasing the statistical accuracy of the data.

Figure 5 Backscatter energy spectrum, with background removed, for the oxygen in the Nb_2O_5 layer of an unannealed sample. Calculations show the layer to contain 6.73×10^{17} oxygen atoms/cm^2. The profile has a uniformity of about ±5%. The curves shown in this and the next two figures have been traced from photographs of computer-generated graphic displays.

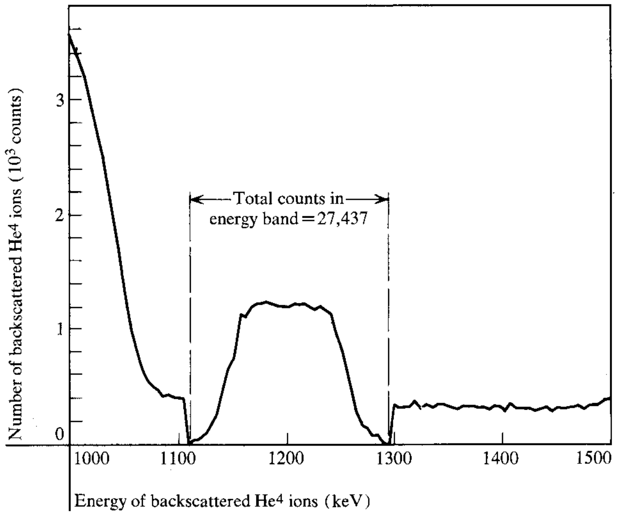

Another sample, similar to the previous one, was annealed at 450°C. The thermal treatment resulted in the oxygen profile shown in Fig. 7. Stoichiometric calculations produced O/Nb values of 3.3/2 and 0.8/2 at the Bi and Nb interfaces of the oxide layer, respectively, indicating that this sample was oxygen-poor with respect to the previous sample. However, the concentration of oxygen had increased to 7.3×10^{17} atoms/cm^2, and the concentration of niobium in the oxide increased from

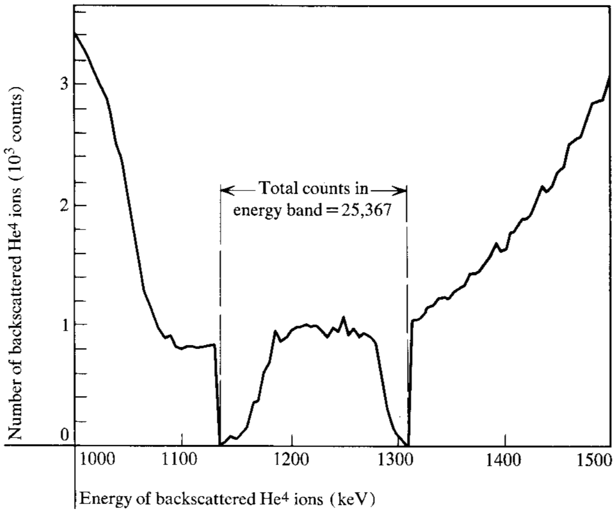

Figure 6 Backscatter energy spectrum, with background removed, for the oxygen in the Nb_2O_5 layer of sample annealed at 375°C. Compared with the unannealed sample of Fig. 5, there has been a slight loss of oxygen, but the oxygen-niobium stoichiometry remains 5/2.

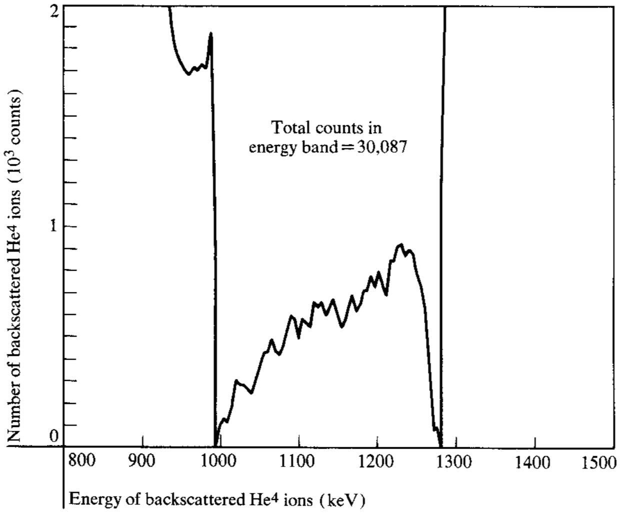

Figure 7 Backscatter energy spectrum, with background removed, for the oxygen in the Nb_2O_5 layer of sample annealed at 450°C. The oxygen-niobium stoichiometry is not uniform, being 3.3/2 at the bismuth interface and 0.8/2 at the niobium interface. However, the total oxygen has increased 12% compared with the sample of Fig. 5.

Figure 8 Scanning electron micrograph of sample annealed at 450°C. (a) Bismuth whiskers about 1 μm long were formed; (b) etching removed the whiskers and about 145 Å of the oxide layer.

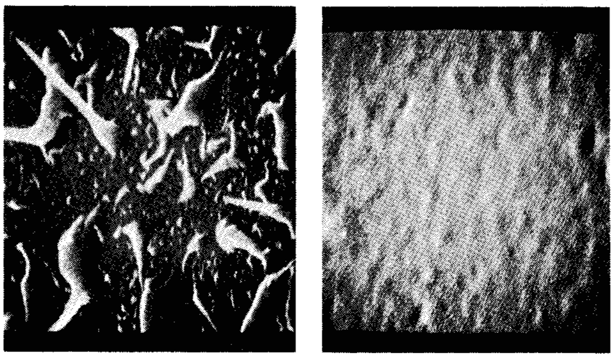

(a) (b)

Figure 9 Concentration profile showing traces of bismuth in the oxide layer of sample annealed at 450°C. The profile was derived from backscatter energy spectrum obtained after bismuth whiskers were etched away.

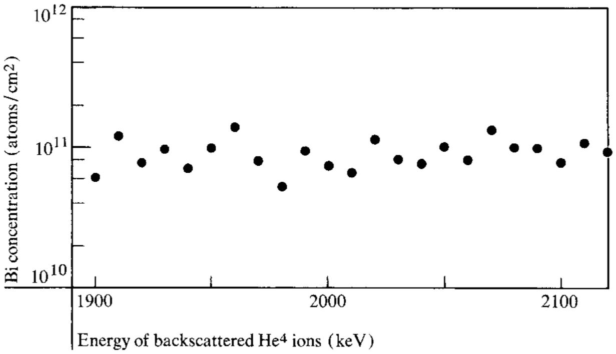

2.7×10^{17} to 7.7×10^{17} atoms per cm^2 compared to the untreated sample.

X-ray analysis of the heat-treated samples showed that a reduction reaction had taken place at the interface between the Nb and Nb_2O_5 layers. In the sample treated at 450°C, reduction had proceeded to the point of forming oxygen compounds such as NbO in the Nb layer and had depleted the oxygen content of the original oxide layer. The decrease of oxygen at the surface of the oxide layer, despite the presence of 50 ppm of oxygen in the heat-treatment atmosphere, was ascribed to the gettering effect of the bismuth layer. The x-ray data showed that the Bi layer did not oxidize completely and that small amounts of Bi_2O_5 were present in the Nb layer.

- *Bismuth*

It was assumed prior to analysis that bismuth would diffuse into the oxide layer during heat treatment. A scanning electron microscope photograph of the bismuth surface after heat treatment at 450°C is shown in Fig. 8(a). The spikes appearing in the photograph were formed from the originally smooth bismuth layer during heat treatment. Since these spikes would distort the results of a backscattering analysis, they were removed by chemical etching. A photograph of the surface after etching is shown in Fig. 8(b). Calculations based on backscattering data revealed that etching had removed about 145 Å (about 11 percent) of material from the oxide layer. The backscattering data, converted to units of bismuth concentration, are given in Fig. 9 for the range corresponding to the expected energies of ions scattered from bismuth atoms. From these data it seemed safe to conclude that fewer than 3×10^{11} atoms/cm^2 of bismuth penetrated deeper than 145 Å into the oxide layer during thermal treatment.

It should be noted that Ref. 3 indicated that some interfacial electrical effects occur in the oxide layer at depths of 50 to 100 Å from the bismuth electrode. Since the etching process in the experiments reported here removed 145 Å from the oxide, the region very near the interface was not analyzed.

Conclusions

Nuclear backscattering has been found to be a useful tool for analyzing films up to 2000 Å thick. The technique has been used to derive concentration profiles for the constituent elements in a complex thin-film structure, and it has provided data for calculating stoichiometry as a function of depth in the film layers. In the experiments reported in this communication, stoichiometry and concentration calculations were accurate to within ten percent. Subsequent improvements in the experimental procedures have improved the accuracy to one percent. A major advantage of the backscattering technique is that it can yield highly accurate results without the need to compare concentration values with those obtained from a calibration sample.

In the study of Nb_2O_5, it was shown that thermal treatment at 450°C caused the oxide to become severely nonstoichiometric and produced the formation of oxygen compounds in the Nb layer through a presumed reduction reaction at the interface. The interface reaction, which proceeds at a rate too fast for fine control, is thought to be the mechanism responsible for the drastic change in electrical properties discussed by other authors. It was also concluded from the experimental study that if bismuth has an effect on the electrical properties of the oxide in an annealed structure, it does so only at very low concentration levels.

References and note

1. T. W. Hickmott and W. R. Hiatt, *Solid State Electronics* **7**, 1033 (1970).
2. S. Basaviah and K. C. Park, *IEEE Trans. Electron Devices*, to be published.
3. R. B. Laibowitz and A. A. Levi, "Dielectric Relaxation and Electron Tunneling in Niobium Oxide," in *Conduction in Low Mobility Materials*, Taylor and Francis, Ltd., London 1971, p. 63.
4. A. Hiraki, M.-A. Nicolet, and J. W. Mayer, *Appl. Phys. Lett.* **18**, 178 (1971).
5. S. T. Picrauz and F. L. Vook, *Appl. Phys. Lett.* **18**, 191 (1971).
6. The corrections for stopping power have been omitted since they were quite small for the experiments discussed here (about two percent) and their derivations would add undesired complexity to the explanation of the experimental analysis.

Received February 15, 1972

The authors are located at the IBM Thomas J. Watson Research Center, Yorktown Heights, New York 10598.